FULL PAPER

Atmospheric pulsed plasma copolymerization of acrylic monomers: Kinetics, chemistry, and applications

Maryline Moreno-Couranjou[1] [ID] | **Jérôme Guillot**[1] | **Jean-Nicolas Audinot**[1] | **Jérôme Bour**[1] | **Emilie Prouvé**[2,3,4] | **Marie-Christine Durrieu**[2,3,4] | **Patrick Choquet**[1] | **Christophe Detrembleur**[5]

[1]Department of Materials Research and Technology, Luxembourg Institute of Science and Technology (LIST), Belvaux, Luxembourg

[2]Laboratoire de Chimie et Biologie des Membranes et Nano-Objets, UMR5248 CBMN, Université de Bordeaux, Pessac, France

[3]CNRS, CBMN UMR5248, Pessac, France

[4]Bordeaux INP, CBMN UMR5248, Pessac, France

[5]Department of Chemistry, Center for Education and Research on Macromolecules (CERM), CESAM Research Unit, University of Liège, Liège, Belgium

Correspondence
Maryline Moreno-Couranjou, Department of Materials Research and Technology, Luxembourg Institute of Science and Technology (LIST), 41. rue du Brill, Belvaux, L-4422 Belvaux, Luxembourg.
Email: maryline.moreno@list.lu

Abstract

In this study, dimethylacrylamide (DMA) homopolymer and DMA/ethylene glycol dimethacrylate (DMA/EGDMA) copolymers are produced by an atmospheric pulsed plasma deposition technique. Such a mild deposition method is used to limit monomer fragmentations and favor cross-linked structures formed through the unsaturated carbon double bond polymerization. The kinetics of deposition, and the dependence of the chemical and physical properties of the films on the comonomer ratio are investigated by combining surface and volume-sensitive techniques. In addition, water-stable catechol-bearing terpolymer films are easily produced from a precursor mixture composed of dopamine methacrylamide dissolved in a 50 mol% DMA/EGDMA solution. Finally, it is demonstrated that the developed coatings can be exploited for efficient one-step bioconjugation reaction for potential biological applications.
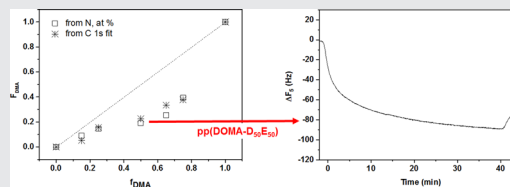
KEYWORDS
atmospheric pulsed discharge, matrix-assisted laser desorption/ionization mass spectrometry, plasma copolymerization, surface modification, water-stable catechol-bearing polymers

1 | INTRODUCTION

Among the various existing techniques for coating a material surface with an organic functional thin film, plasma enhanced chemical vapor deposition (PECVD), also known as plasma polymerization, has gained considerable interest at laboratory and industrial levels. Indeed, PECVD presents several unique advantages, such as being a solvent- and catalyst-free, up-scalable, and substrate-independent technique, allowing the fast production of high-purity organic coatings.[1] By selecting the monomer nature and adjusting the process deposition conditions, easy tuning of the coating property and chemistry can be achieved.[2,3] However, plasma polymer deposition involves complex and multiple processes, such as radical and ionic chain growth polymerization, ion-molecule reactions, monomer fragmentation–polyrecombination, plasma-surface etching, and so on.[4] As a consequence, plasma polymerized films (PPFs), known as "plasma polymers," often lack the regular repeat units found in conventional polymers.[5,6] As the plasma is capable of monomer fragmentation, it might reduce the incorporation of desired functional groups into the films and can also result in branching and/or undesirable high degrees of crosslinking.[1] To limit the negative plasma impacts on the monomer structure, different routes have been employed relying on: (a) decreasing the discharge energy by igniting discharges in helium atmosphere[7]; (b) using a postdischarge configuration[8]; and/or (c) pulsing of the plasma discharges.[9,10] Förch et al.[11] characterized the mechanism of pulsed plasma deposition in terms of plasma on-time (t_{on}), plasma off-time (t_{off}), and input power, (P_{peak}). The plasma on-time to the total cycle time ratio (i.e., $t_{on}/(t_{on} + t_{off})$) is defined as the duty cycle (DC). Films deposited at low DC are generally characterized by a high functional retention of the monomer as well as a low crosslinking degree.[12]

During the last few decades, engineering biointerfaces involving plasma polymers have gained considerable interest for various biomedical applications, such as biosensing, tissue engineering, bioimplants, and so on.[13,14] In this field of application, the covalent immobilization of bioactive molecules on PPF interfaces in aqueous media through reactions with reactive chemical moieties, such as amino, carboxyl, epoxy groups on the surface, is generally targeted.[15] Recently, the deposition of PPF-bearing catechol/quinone groups has been reported by using a two-step atmospheric liquid-assisted plasma polymerization approach. The method relied on the deposition of a liquid precursor mixture onto a surface followed by a plasma curing step.[16] Compared to amino or carboxyl functionalized surfaces, these catechol-bearing surfaces ensure the one-step covalent immobilization of biomolecules carrying amino or thiol groups through Michael addition and/or Schiff base formation.[17]

However, the production of such reactive, yet water-stable, PPFs still represents a technological challenge; as achieving a balance between the functional group density and the film's stability (i.e., film crosslink density) is not trivial.[18] Upon storage, among all PPFs, amino-functionalized films are particularly known to undergo hydrophobic recovery (in air), post-plasma oxidation (in air and in water), as well as major surface restructuring and film loss (in water).[6]

To circumvent this limitation, different strategies have been developed. PPFs have recently been synthesized via direct in situ monitoring of the plasma power during film growth. Such particular deposition conditions result in a vertical chemical gradient from a highly cross-linked/less functional to a less cross-linked/highly functional plasma polymer film with an overall thickness of around 20 nm.[6,19] Another approach relies on the combination of plasma polymerization and ion implantation technique. Such radical-functionalized plasma polymers have been reported to allow the efficient covalent immobilization of fibronectin or bone morphogenetic protein 2, leading to stable biomimetic interfaces for bone implant applications.[18] Finally, PPFs can be produced from co-injection of monomers, also known as plasma copolymer formation. In such an approach, two kinds of monomers are mainly exploited, namely functional and difunctional unsaturated vinyl-based compounds. Homofunctional monomers can rely on vinyltrimethoxysilane (VTMOS).[2] In the case of VTMOS, the post-hydrolysis of the methoxy groups of the siloxane and silanol condensation leads to a network cross-linked via Si–O–Si linkages. Among difunctional crosslinkers, N,N′-methylenebisacrylamide[20,21] and ethylene glycol dimethacrylate (EGDMA)[22–24] are mainly used, in composition ranging from around 2[20,22,23] up to 20 mol%.[24] To a lesser extent, glycidylmethacrylate is also reported based on two reactive functionalities, that is, an acrylate carbon–carbon double bond and an epoxide ring group.[25]

In a previous work, the capabilities of an atmospheric aerosol-assisted pulsed plasma polymerization process, involving a homemade dopamine acrylamide (DOA) monomer and 2-hydroxyethyl methacrylate (HEMA), used as solvent and comonomer, were successfully reported for the deposition of tunable catechol-bearing films in term of thickness, morphology, and catechol density.[26] In particular, it was demonstrated that a pulsed discharge defined by a 0.2% DC (i.e., 1:400 ms as t_{on}:t_{off} ms) ensured the formation of smooth and catechol-enriched

films. Hence, this one-step deposition route offers an interesting alternative to the liquid-assisted polymerization route that might suffer from limitations related with surface tension effects, such as wetting limitations. Nevertheless, the developed DOA–HEMA based coatings presented a lack of stability in aqueous media, excluding their exploitation as biointerfaces.

Hence, one objective of this study was to exploit atmospheric pulsed plasma copolymerization for producing water-stable catechol-bearing coatings useful for potential biological applications by promoting one-step bioconjugation reaction. Considering the universality of the developed approach applicable to any vinyl-based monomers, here, commercial solid dopamine methacrylamide (DOMA) was used instead of DOA as a catechol precursor. N,N-dimethylacrylamide (DMA) was selected as a comonomer for its good DOMA solubilization property. EGDMA was used as a crosslinker agent to form water-stable films. To easily produce water-stable DOMA/DMA/EGDMA terpolymer films, the study was divided into three successive steps. Efforts were first made to optimize pulsed DMA-homo-plasma polymerization ensuring a well-retained monomer structure in the deposited film. It is now well established that a short t_{on} efficiently produces initiating species, among others radicals, whereas long t_{off} periods promote the propagation of the free-radical polymerization reaction.[27] Therefore, particular attention should be paid when selecting the plasma off-time duration as the latter should be in accordance with the lifetime of the monomer radical species considered. Hence, the first section of the work aimed at investigating the optimal t_{off} considering plasma DMA homopolymerization. Indeed, in the final stage, DOMA, dissolved in DMA, has been co-polymerized in the presence of a bifunctional crosslinker monomer, to improve water-resistance property. Later, the growth mechanism of DMA/EGDMA copolymerization was investigated mainly through kinetics, chemical and physical analyses. In addition, to properly envision DMA/EGDMA-based copolymers as biomimetic interfaces, indirect cytotoxicity tests involving human mesenchymal stem cells (hMSCs) were carried out. At last,

from the acquired knowledge, water-stable catechol-bearing coatings were produced and successfully exploited for strong covalent immobilization of lysozyme used as a model biomolecule.

2 | EXPERIMENTAL

2.1 | Materials

All chemical monomers, depicted in Figure 1 and including DMA (Sigma-Aldrich), EGDMA (Sigma-Aldrich), DOMA (Specific Polymers), and lysozyme (L6876; Sigma-Aldrich) were used as received. Acetone, ethanol (technical grade), and Dulbecco's phosphate-buffered saline (DPBS; 1X) solutions were purchased from VWR International. Silicon wafers (Siegert Wafer), aluminum foils (200-mm thick foil [Ra: 0.2 mm] of a 8xxx alloy, Eurofoil) and Au-QCM-D sensors (Quartz Pro AB) were used as substrates. The latter were cleaned via successive ultrasonic washings in acetone and ethanol and further dried under a nitrogen flux. Optical quartz glass pieces (Präzisions Glas & Optik) were used as received as substrates for ultraviolet (UV) analyses. Before plasma deposition, all substrates were cleaned and activated using a 95%/5% argon/oxygen plasma ignited by a 10 kHz sinusoidal electrical excitation (SOFTAL generator) operating at 1.6 W/cm^2 in a 1.6% DC. This plasma pretreatment step allowed the removing of organic impurities present at the surface of the substrates and ensured a good anchoring of the deposited film.

2.2 | Atmospheric plasma depositions

Thin films were deposited using an open-air atmospheric pressure dielectric barrier discharge (AP-DBD) process depicted in Figure 2. The discharge was produced between two plane-parallel high voltage electrodes covered by alumina and a moving table as the ground electrode, thus generating an approximately 19 cm^2 plasma discharge area. Samples were placed on the moving table
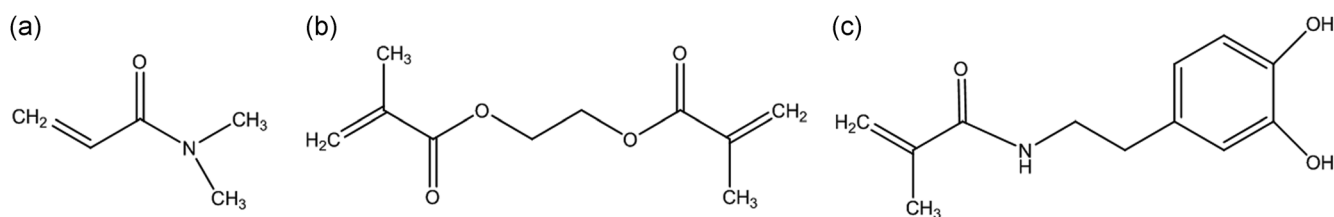

FIGURE 1 Chemical schemes of (a) liquid N,N-dimethylacrylamide (DMA), (b) liquid ethylene glycol dimethacrylate (EGDMA), and (c) solid dopamine methacrylamide (DOMA)
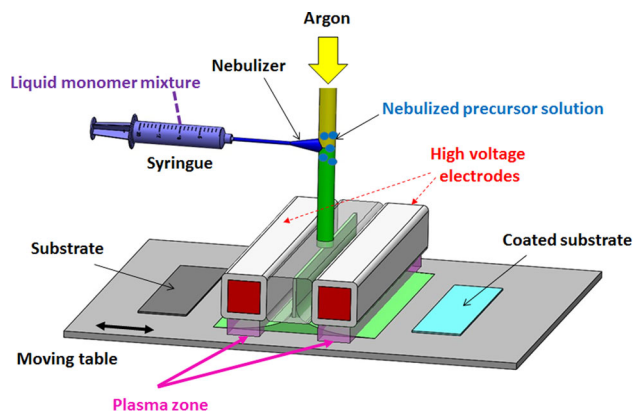
FIGURE 2 Scheme of the atmospheric pressure dielectric barrier discharge set-up

and the electrode gap adjusted at 1 mm. The total process gas flow was fixed at 20 slm of argon (99.999%; Air Liquide). All experimental depositions have been carried out using a 10 kHz sinusoidal signal and a 1.6 W/cm^2 power density. The t_{on} duration was fixed at 1 ms to limit the monomer fragmentation. The precursor solution was nebulized using a OneNeb injector system (Agilent) and a syringe pump to control its flow delivery (5 μl/min). Different precursor solutions were used, namely (a) pure DMA or pure EGDMA to produce the corresponding homopolymer; (b) DMA–EGDMA liquid mixtures prepared at different DMA and EGDMA molar concentrations; and (c) DOMA (80.5 mg/ml in DMA) in 50 mol% DMA/EGDMA solution to synthesize the terpolymer. Later, films issued from DMA/EGDMA mixtures will be referenced as $D_xE_{(1-x)}$ with x as the DMA molar fraction in the liquid mixture.

2.3 | Thin film characterizations

Scanning electron microscopy (SEM) images were taken using on a FEI Quanta 200F (Zürich, Switzerland).

The film growth rates were determined from the coating thicknesses measured by ellipsometry (FS-1 model; Film Sense), using a Cauchy function for fitting, divided by the synthesis process duration.

The surface topography of the different films was characterized by means of an atomic force microscope (AFM) Asylum MFP-3D Infinity in an amplitude modulation tapping mode. The selected tip was the reference ACT160TS (26 N/m) from Olympus. The topography was recorded by keeping the amplitude of the cantilever first resonance frequency at 60 nm from a 80 nm free amplitude. Images of 512 pixels × 512 pixels were recorded at a line speed of 1 Hz. The data treatment was performed with the Asylum Research software. The arithmetical

roughness parameter values (Sa) were extracted after the removal of the mean plane.

The optical absorbance of the films deposited on quartz substrates was measured in the range of 200–800 nm using a UV-Vis-NIR spectrophotometer (Lambda 950; PerkinElmer) with a 150-mm diameter integrating sphere.

Fourier-transform infrared (FTIR) measurements were performed on a Bruker Hyperion 2000 microscope using the attenuated total reflectance (ATR) mode. The apparatus is composed of an ATR objective with a germanium crystal and a liquid nitrogen-cooled mercury cadmium telluride detector. Spectra were acquired from 32 scans at a 4 cm^{-1} resolution. The data treatment was done using the OPUS software.

X-ray photoelectron spectroscopy (XPS) measurements were carried out on a Thermo Fisher K-Alpha spectrometer using a monochromatic aluminum source (1,486.6 eV). The size of the X-ray beam was 200 μm. The C 1s, O 1s, and N 1s narrow spectra were acquired with a constant pass energy of 20 eV. A flood gun combining both low energy argon ions and electrons was used during the measurements. The curve fitting was performed with the commercial CasaXPS software (version 2.3.19).

Atmospheric pressure matrix-assisted laser desorption/ionization high-resolution mass spectroscopy (AP-MALDI-HRMS) spectra measurements were performed on an AP-MALDI UHR source (MassTech Inc.) coupled to an LTQ/Orbitrap Elite from Thermo Fisher Scientific. 2,5-Dihydroxybenzoic acid diluted in methanol was selected as the matrix. A total of 1 μl of the matrix was then spotted on the thin films to form a co-crystal with the soluble part of the film when the methanol is evaporated. Electrospray ionization (ESI) mass spectrum (MS) was recorded with an LTQ/Orbitrap Elite mass spectrometer coupled with an Ion Max source, equipped with an electrospray probe from Thermo Fisher Scientific. First, the plasma polymer coating was dissolved in methanol and secondly diluted with a methanol solution of ammonium acetate (10 mmol/L). This so-obtained solution was directly infused at a flow rate of 10 μl/min using a syringe pump. A voltage of 2 kV and a temperature of 300°C were applied to the metal capillary. A coaxial sheath gas, as well as auxiliary gas (dry He), were used with flow rate of 40 and 10 (arbitrary unit), respectively, to favor nebulization. Hence, ESI-MS analyses allowed to characterize the soluble part (i.e., extract) of the plasma polymer film in methanol.

Water contact angle (WCA) measurements were carried out using a Krüss DSA100 apparatus. For each sample, at least six water droplets of 2 μl volume were deposited at different positions. The WCA evolution was followed up via multiple analysis of the live video images

acquired for 10 s at a frequency of 2 fps. The WCA value was obtained from the droplet shape using a numerical fit based on the ellipse (Tangent 1) model.

Real-time immobilization of lysozyme onto the surface of coated sensors (Ti X-cut resonators with a 4.95 MHz resonant frequency) was investigated by the quartz crystal microbalance with dissipation monitoring (QCM-D) technique using a Q-Sense Explorer system (QSense, Biolin Scientific). Sensors coated with a 100-nm thick pp(DOMA-$D_{50}E_{50}$) or pp($D_{50}E_{50}$) film were investigated. The DPBS solution flow rate was fixed at 100 μl/min and the system were allowed to equilibrate, achieving a stable baseline. A 10 mg/ml Lsz DPBS solution at pH 7.2 was introduced and the frequency (Δf) shift parameter of all the detected harmonics monitored to provide insights into the mass of lysozyme adsorbed.

2.4 | Biological tests

hMSCs are used to evaluate the cytotoxicity of the materials. hMSCs were obtained from PromoCell (Germany). Cells were then cultured in Mesenchymal Stem Cell Growth Medium 2 (PromoCell) and incubated in a humidified atmosphere containing 5% (vol/vol) CO_2 at 37°C. All cells were used at passage number 5, were subconfluently cultured, and were seeded at 6,000 cells/cm^2. For all cytotoxicity assays, silicon wafer was used as a negative or noncytotoxic control. Cells cultured under normal, or blank, conditions and without any material were used as control. A solution of culture media containing 64 g/L of phenol was used as a cytotoxic control. Following ISO standard 10993-5, extract tests have been performed to evaluate whether there is a cytotoxic response to the materials. The extract test evaluates the cytotoxicity of any leachable byproducts from the material. Cells were plated and grown to 80% confluency before initiating the assay. The materials (silicon and silicon coated with a $D_{15}E_{85}$ thin film) were incubated with Mesenchymal Stem Cell Growth Medium 2 culture media at a concentration of 3 cm^2/ml for 72 hr. After 72 hr, the cell culture media was removed and replaced with the full extract media or with diluted extract media with fresh culture media at 50%, 10%, and 1%. Cells were then incubated at 37°C and 5% CO_2 for 24 hr before cytotoxic evaluation with 2,3-bis-(2-methoxy-4-nitro-5-sulfophenyl)-2H-tetrazolium-5-carboxanilide (XTT) cell metabolic activity assay. For the cytotoxic control, the culture media was removed and replaced by a culture media containing 64 g/L for 24 hr. Before cytotoxicity evaluation, the media was placed in a separate well plate to avoid phenol evaporation and interaction with the cells in the surrounding wells.

The Cell Proliferation Kit II (XTT; Roche, Mannheim, Germany) was used to quantitatively evaluate the cell metabolic activity. XTT was used according to the manufacturer's protocols. The electron coupling and XTT labeling reagents were thawed and immediately combined in a 1:50 μl ratio. Then the XTT solution was added to the cell culture wells, 75 or 150 μl for a 96-well plate. Absorbance was measured at 450 and 630 nm after 18 hr of incubation at 37°C with a ELx808 Absorbance Microplate Reader (BioTek Instruments). Net absorbance was calculated ($A_{450} - A_{630}$) for each sample of the five biological replicates. The relative cell metabolic activity was normalized to the mean of the blank culture media. Samples were evaluated, and the mean cell metabolic activity and standard deviations were reported ($n = 5$).

3 | RESULTS AND DISCUSSION

3.1 | Pulsed plasma homopolymer deposition from DMA

Irrespective of the t_{off} duration ranging from 10 to 200 ms, for a fixed 1 ms t_{on}, the top view SEM observations revealed the formation of particle-free and pinhole-free films (Figure S1). Complementary AFM measurements (Figure 3), carried out on 37 ± 6 nm thick coatings, indicated that the films were smooth and covered homogeneously all the surfaces of the substrates.

The plot of the film growth rate per discharge pulse as a function of t_{off} is reported in Figure 4a. Interestingly, the curve was characterized by an increased layer growth for t_{off} values ranging from 10 to 60 ms and followed by a plateau, indicating a blocking in the plasma polymerization. In Figure 4b, the evolution of the film thickness is reported as a function of the t_{off} duration for a fixed 1 ms t_{on} and an effective plasma exposure time fixed at 3 s. Such plot tends to confirm the existence of a plateau in the layer growth. By varying the t_{off} values from 10 up to 60 ms, the film thickness was progressively increasing, suggesting that film growth occurred during these plasma off periods. Similarly, it was observed that for t_{off} values higher than 60 ms, the film thickness remained quite constant, corroborating with the termination of the plasma polymerization reactions.

The effects of the t_{off} duration on the chemistry of the films were investigated by FTIR analysis shown in Figure 5. Before plasma polymerization, DMA molecule exhibited different characteristic infrared bands: (a) [A] at 3,100 cm^{-1}, H–C=C stretching mode, [B] at 2,933 cm^{-1}, $(CH_3)_2$ symmetric stretching; (b) [C] very strong band at 1,646 cm^{-1}, (C=O, amide band I) stretching mode; (c) [D] strong band at 1,609 cm^{-1}
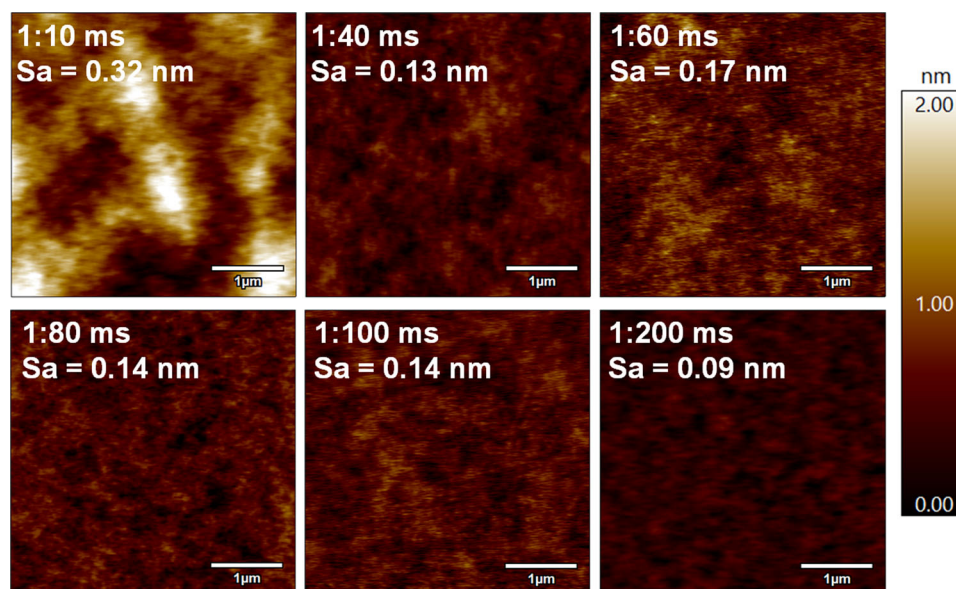
FIGURE 3 Atomic force microscope pictures of pulsed plasma polymers deposited on silicon substrates from *N,N*-dimethylacrylamide at a fixed 1 ms t_{on} and different t_{off} durations. The arithmetical mean height (Sa) is indicated

(C=C); (d) [E] at 1,494 cm^{-1} (C–N, amide band III) stretching; (e) [F] double bands at 1,418 and 1,401 cm^{-1}, N–(CH$_3$)$_2$ bending mode; (f) [G] at 1,259 cm^{-1}, C–N in N(CH$_3$)$_2$ asymmetric stretching mode; (g) [H] and [I] at 1,143 and 1,053 cm^{-1}, respectively, N–(CH$_3$)$_2$ rocking mode. Atmospheric pulsed plasma polymerization induced the consumption of the H–C=C bond [A] and the retention of the amide bond, noticeable with the presence of the fingerprints bands of DMA, namely [C′] (i.e., C=O shifted at 1,623 cm^{-1}), [E], [G]. Such chemical retention result might be correlated to the amide alpha position to the DMA-vinyl bonds. Indeed, in the literature, the existence of resonance is reported as a stabilizer of a chemical functional group limiting its fragmentation.[28] However, it is worth noting that the plasma polymerization also induced part of monomer fragmentation, probably during the plasma ON time, such period being characterized by a plasma gas phase enriched in damaging species such as electrons, ions, radicals, and UV photons. Hence, DMA-pulsed polymerized films also contained novel functional groups, noticeable with the broad [C′] band and the appearance of the [J] and [K] bands, around 3,400 cm^{-1} and at 1,711 cm^{-1}, related to NH/OH and aldehyde/ketone/carboxylic acid groups, respectively.
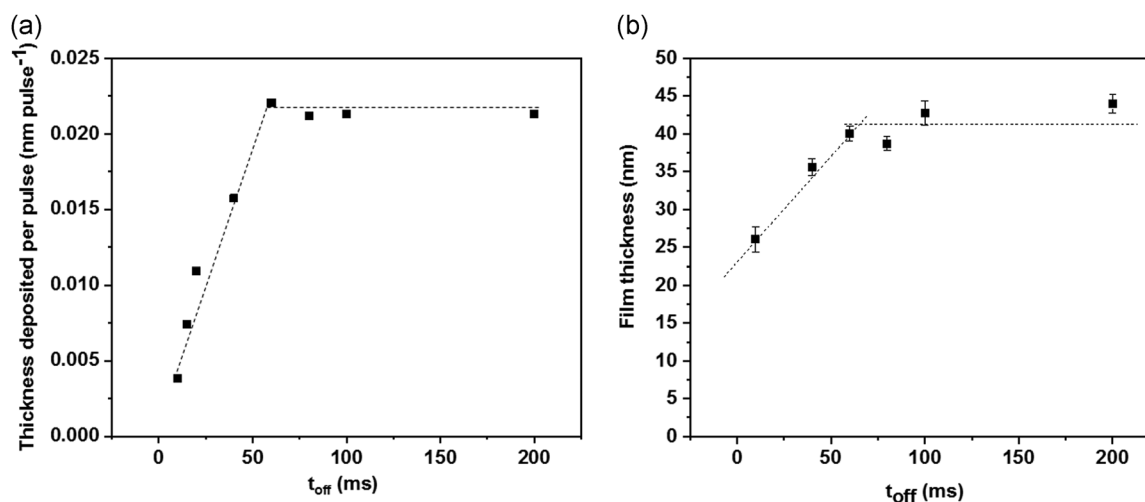

FIGURE 4 (a) Film thickness deposited per pulse as a function of t_{off} duration for different effective plasma exposure durations and (b) evolution of the film thickness as a function of the t_{off} duration for an effective plasma exposure fixed at 3 s
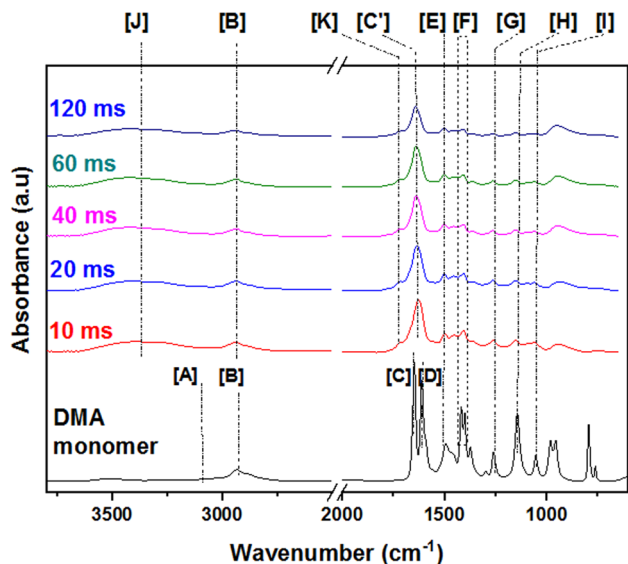
FIGURE 5 Infrared spectra of *N,N*-dimethylacrylamide (DMA) monomer and DMA plasma polymer films deposited at a fixed 1 ms t_{on} and different t_{off} ranging from 10 to 120 ms

To gain further insights into the film surface composition and chemistry, XPS analyses were carried out. Irrespective of the t_{off} values, the elemental composition of the films remained almost constant (Figure 6a). One can notice that the N/C ratio of the polymer was around 0.2 and corresponded to the stoichiometric ratio in the monomer structure whereas the O/C values in the film were slightly higher than in the monomer (0.23 vs. 0.20) maybe due to the incorporation of few oxygen. Considering the open-air configuration of the plasma rector, this might originate from the reactivity of oxygen and water emanating from the surrounding atmosphere. Another possibility could be that, after the deposition, free radicals entrapped in the polymer film easily reacted with atmospheric oxygen.

By comparing the different XPS elemental core level envelopes, it was observed that, irrespective of the t_{off} values, the C, N, and O chemical environments of the different films were similar. Indeed, as reported in Figure 7, one can notice that there was a perfect overlap of the C 1s, O 1s, and N 1s core level envelopes.
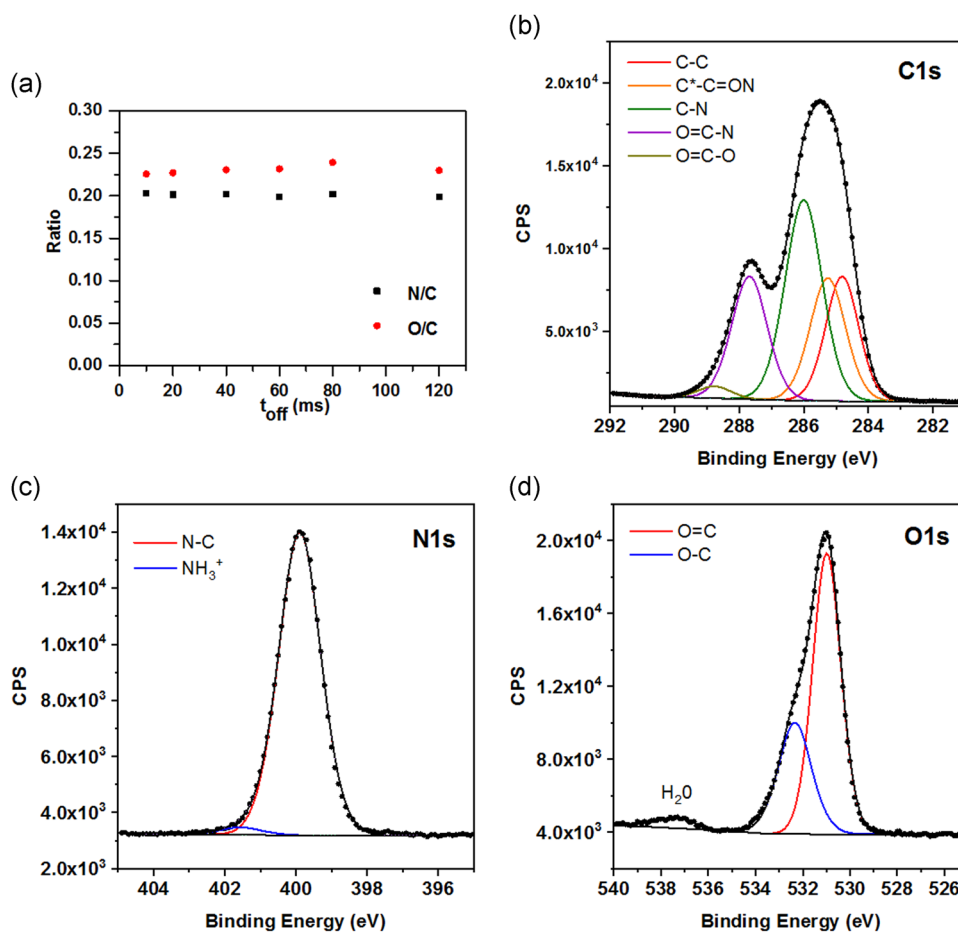

FIGURE 6 *N,N*-dimethylacrylamide (DMA) plasma homopolymers. (a) Stoichiometric ratios in the function of t_{off} duration for a 1 ms t_{on} and X-ray photoelectron spectroscopy curve fitting for (b) C 1s, (c) N 1s, and (d) O 1s of DMA-homopolymer deposited at 60 ms t_{off} and 1 ms t_{on}
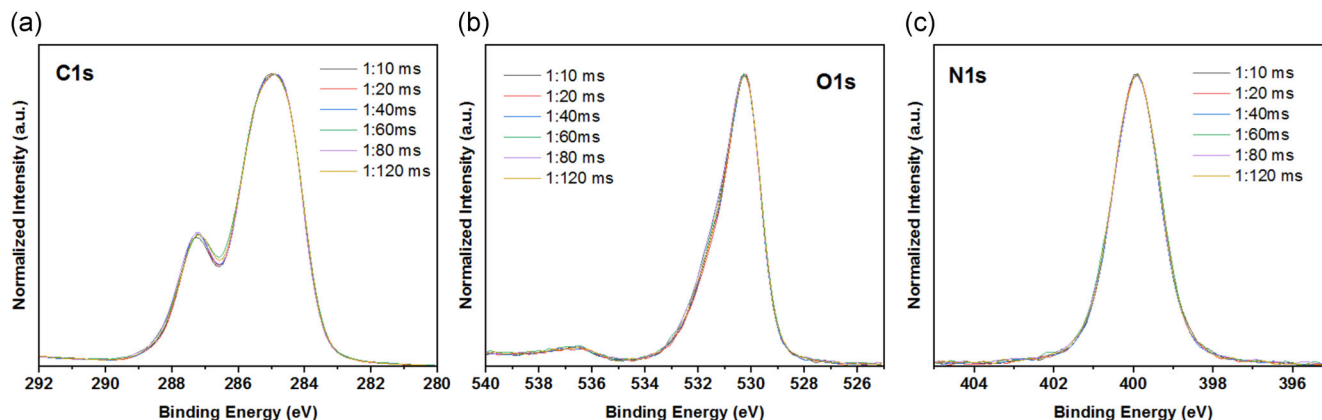
(a)

(b)

(c)

FIGURE 7 X-ray photoelectron spectroscopy (a) C 1s, (b) O 1s, and (c) N 1s core level envelopes of *N,N*-dimethylacrylamide-homopolymers deposited at a fixed 1 ms t_{on} and t_{off} values ranging from 10 to 120 ms

The C 1s peak, reported in Figure 6b, was fitted with four main components corresponding to the expected chemical environments for the carbon atoms in poly (DMA)[29] namely: C–C at 284.80 eV, C*–C=O at 285.25 eV, C–N at 286.0 eV, and N–C=O at 287.7 eV. An additional contribution is present at 288.75 eV and is attributed to carboxylic acid, in accordance with the IR results. The N 1s spectrum, shown in Figure 6c, was centered at 399.9 eV corresponding to nitrogen in the amide group. A second contribution (only 2.5% of the total intensity) was found at 401.6 eV and was attributed to NH_3^+ species. The O 1s line (Figure 6d) was fitted with two peaks at 531.0 and 532.35 eV for the oxygen doubly and singly bonded to carbon atoms, respectively. The presence of water was also detected in every sample, characterized by a broad contribution at 537.4 eV.
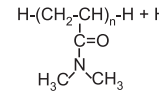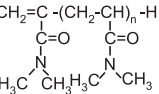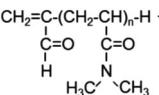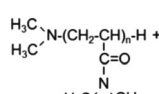
Hence, the kinetic study combined with the AFM, XPS, and FTIR analyses corroborated a film formation from predominant soft heterogeneous chemical polymerization reactions during the t_{off} period. In others words, during these long plasma off times, the film growth tended to be greatly favored by reactions occurring at the surface of the solid substrate with monomer molecules and species (i.e., radicals), formed during the t_{on} time and present in the gas phase. The plasma being off, the surfaces were not impacted by damaging species such as UV, ions, or electrons. In particular, from the film growth study, the DMA radical lifetime was estimated around 60 ms. This stood for the optimal t_{off} value, as film growing (i.e., propagating reactions) stopped for higher duration. Considering that fresh monomer molecules were continuously injected into the process reactor, the stopping of the polymerization reactions could not be attributed to an impoverishment of monomer in the gas phase. In fact, during the t_{on} period, the plasma-monomer interactions induced the formation of radical species that might freely play the role of initiating, terminating group, or simple vinyl adducts. Therefore, the ending of the polymerization might be due to the reaction of some terminating species with the growing film.

To gain further insights into the molecular composition of the coating deposited in a pulsed 1:60 ms condition, AP-MALDI and ESI coupled to HRMS analyses were performed.

Importantly, both AP-MALDI-HRMS and ESI-HRMS LDI-HRMS analyses provide a partial representation of the film structure. For AP-MALDI-HRMS analyses, a matrix, composed of dihydroxybenzoic acid and methanol, was deposited onto the film surface. The soluble part of the film and the matrix formed a co-crystal when the methanol evaporated. The AP-MALDI-HRMS analysis was done on the specific spotted surface. Concerning the ESI-HRMS analyses, the results are derived from the soluble part of the polymer film in methanol. Table 1 summarizes the main different oligomer distributions detected. The complete corresponding m/z ions are reported in Table S1. Irrespective of the analytical technique employed, four main distributions of oligomers presenting the general formula $[R-(DMA)_n-H + H]^+$ with R being an end group, were detected. The MALDI-HRMS spectrum was mainly dominated by intact oligomers of poly(DMA) proton adducts (i.e., H_1 oligomer in Table 1), corresponding to R as a proton terminal group, $[H(DMA)_nH + H]^+$, up to $n = 11$ repeating units compared with $n = 7$ for ESI-HRMS analyses. In addition, a hydrogen abstraction reaction in DMA might form the terminal end group of the H_2 oligomer family, with n up to 8. Another modification of the DMA monomer might come from the reduction of the amide into an aldehyde group, leading to the formation of $CH_2=C–(C=O)H$ as end group, thus forming the oligomers family H_3, that is, $[CH_2=C(C=O)H-(DMA)_n-H + H]^+$ with n up to 9.

TABLE 1 Main oligomers distributions detected by AP-MALDI and ESI-HRMS analyses of atmospheric pulsed DMA plasma polymerized films.

Annotation	Oligomer formula	Repeating unit, n, from	
		MALDI-HRMS	ESI-HRMS
H_1	H-(CH$_2$-CH)$_n$-H + H]$^+$ C=O N H$_3$C CH$_3$	$2 \leq n \leq 11$	$2 \leq n \leq 7$
H_2	CH$_2$=C -(CH$_2$-CH)$_n$-H + H]$^+$ C=O C=O N N H$_3$C CH$_3$H$_3$C CH$_3$	$1 \leq n \leq 8$	$1 \leq n \leq 6$
H_3	CH$_2$=C-(CH$_2$-CH)$_n$-H + H]$^+$ C=O C=O H N H$_3$C CH$_3$	$1 \leq n \leq 9$	$1 \leq n \leq 7$
H_4	H$_3$C N-(CH$_2$-CH)$_n$-H + H]$^+$ H$_3$C C=O H$_3$C CH$_3$	$1 \leq n \leq 9$	$1 \leq n \leq 7$

Abbreviations: AP, atmospheric pressure; DMA, *N,N*-dimethylacrylamide; ESI, electrospray ionization; HRMS, high-resolution mass spectroscopy; MALDI, matrix-assisted laser desorption/ionization.

Finally, the H_4 oligomer distribution, $[(CH_3)_2N\text{-}(DMA)_n\text{-}H + H]^+$ with n up to 9 was detected, the $(CH_3)_2N$ end group resulting from the bond scission in DMA between nitrogen and the carboxyl group. Two peaks at m/z 100.077 and 117.102 were barely detected, probably related to the presence of a small amount of unreacted DMA monomer in protonated and ammonium adducts, respectively. Compared with ESI-HRMS, MALDI-HRMS appeared as the most appropriate technique, allowing the systematic detection of longer oligomer chains. Such result justifies that the technique was further exploited in the next section of the work.

Complementary water immersion tests indicated that, irrespective of the t_{off} duration, the pulsed DMA-homopolymer films were fully soluble, sign of a lack of crosslink degree in the film network. To produce water-stable DMA-based films, the pulsed plasma polymerization of DMA in the presence of EGDMA, used as crosslinker agent, was investigated. To gain knowledge of the pulsed plasma copolymer growth mechanism, the influence of a broad range of DMA/EGDMA mixture compositions on the final film properties was investigated.

3.2 | Pulsed plasma copolymer deposition from DMA/EGDMA mixtures

The deposition rate of films produced at a 1:60 ms pulsed condition from various EGDMA/DMA precursor
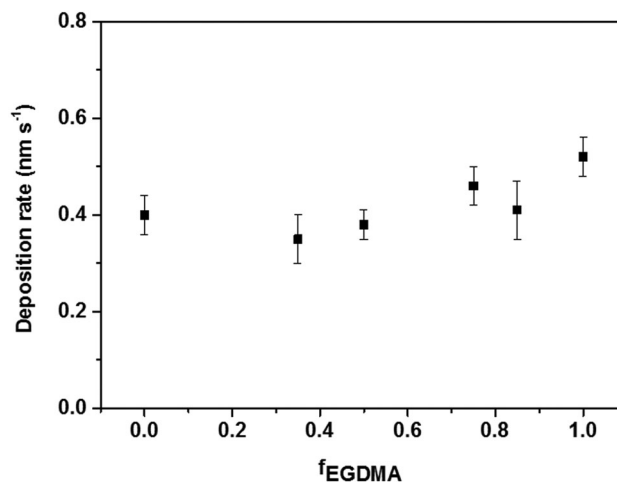

FIGURE 8 Plot of the deposition rate as the molar fraction of EGDMA, f_{EGDMA}, for different DMA/EGDMA mixtures. DMA, *N,N*-dimethylacrylamide; EGDMA, ethylene glycol dimethacrylate

mixtures is reported in Figure 8. The plasma homopolymer from EGDMA ($f_{EGDMA} = 1$) presented a slightly higher deposition rate than the DMA one (i.e., $f_{EGDMA} = 0$), namely 0.52 ± 0.04 vs 0.40 ± 0.04 nm/s. Such result might be explained by the presence of two vinyl groups instead of only one for DMA, thus favoring a double polymerization pathway. In a coherent way, increasing the EGDMA content in the monomer mixtures was accompanied by a slight increase of the film deposition rate.
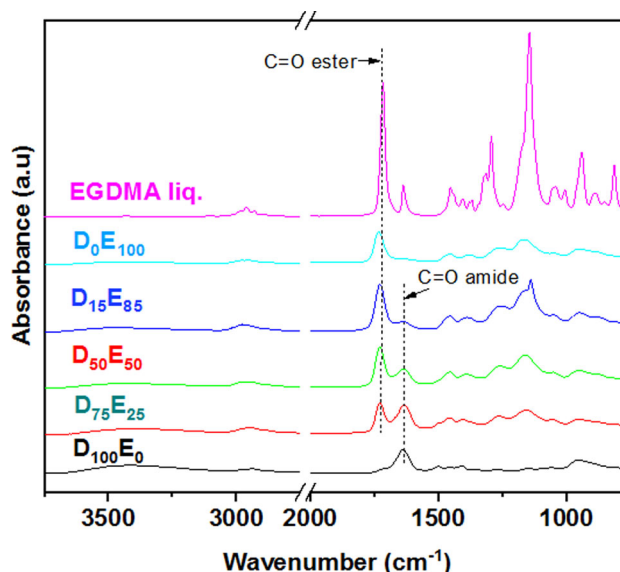

FIGURE 9 Fourier-transform infrared spectra of liquid EGDMA monomer and DMA/EGDMA plasma polymer films deposited from $D_{100}E_0$, $D_{75}E_{25}$, $D_{50}E_{50}$, $D_{15}E_{85}$, and D_0E_{100} precursor mixtures. DMA, *N,N*-dimethylacrylamide; EGDMA, ethylene glycol dimethacrylate

TABLE 2 XPS elemental composition of films synthesized from different monomer feed ratios. As references, theoretical poly(DMA) and poly(EGDMA) compositions are also reported.

Samples	XPS chemical composition (at%)		
	C	N	O
polyDMA (theory)	71.4	14.3	14.3
$D_{100}E_0$	71.1	13.0	16.0
$D_{75}E_{25}$	71.6	3.5	25.0
$D_{65}E_{35}$	73.3	2.2	24.5
$D_{50}E_{50}$	73.1	1.6	25.3
$D_{25}E_{75}$	72.8	1.2	26.0
$D_{15}E_{85}$	72.4	0.7	26.9
D_0E_{100}	72.3	0.2	27.5
polyEGDMA (theory)	71.5	0.0	28.5

Note: As references, theoretical poly(DMA) and poly(EGDMA) compositions are also reported.

Abbreviations: DMA, *N,N*-dimethylacrylamide; EGDMA, ethylene glycol dimethacrylate; XPS, X-ray photoelectron spectroscopy.

The pulsed DMA and EGDMA plasma copolymerization was chemically monitored by FTIR analyses reported in Figure 9. As reference, coating from pure EGDMA was analyzed, highlighting that such polymerization condition induced a strong preservation of the monomer structure, noticeable with the presence of the ester (C(O)O, 1,729 cm^{-1}) and ether (COC, 1,168 cm^{-1}) bands. In addition, irrespective of the monomer mixture compositions, coatings presented the characteristic ester and amide bands, thus confirming the good EDGMA and DMA incorporation into the plasma copolymer chain backbone.

To gain insights into the film surface composition, XPS analyses were carried out. Table 2 summarizes the XPS elemental composition and contributions of films produced from pure DMA and EGDMA and different DMA/EGDMA mixtures. As references, theoretical compositions of conventional DMA and EGDMA polymers are also reported. Interestingly, film deposited from pure EGDMA presented a composition close to the theoretical one. A negligible amount of nitrogen (around 0.2 at%) was also detected, probably from a slight nitrogen surface adsorption or incorporation during the film synthesis. Therefore, nitrogen was considered as the DMA fingerprint for quantification purpose. Hence, using a precursor mixture composed of 50 mol% of DMA and EGDMA leads to a film (i.e., $D_{50}E_{50}$) containing only 1.6 at% of nitrogen, which is four times below the expected amount (i.e., 6.5 at%) considering a linear behavior. All in all, irrespective of the DMA amount in the feed, poor nitrogen content was detected, highlighting a poor incorporation of DMA in the film.

To confirm the film surface composition, XPS C 1s curve fittings were carried out to determine the proportion of each polymer in the film. However, a particular methodology relying on considering the mutual contribution of global C 1s envelops from pure DMA and EGDMA homopolymer films was applied (Figure 10). Indeed, the XPS peaks of polymers are usually fitted with a set of synthetic Gaussian/Lorentzian components corresponding to the various functions or chemical environments of the considered element, but this method requires strict constraints between the peaks parameters to obtain reliable results in complex systems. In this study, the C 1s spectra of the copolymerized films were fitted with only two components corresponding to the monomer contribution, the synthetic components being replaced, in the CasaXPS software, by the experimental lineshapes obtained on pure DMA and EGDMA films. This peak fitting procedure is not only simple and fast but it also allows the combination of experimental envelope with eventual additional synthetic components for functional groups not present in the initial monomers to provide robust results. Interestingly, excellent fits were obtained by considering only the EGDMA and DMA individual envelope. Hence, the plasma copolymerization of DMA and EGDMA in different proportions did not create novel species in the films. Considering the work of Beck et al.,[30] such result was not predictable. Indeed, the authors reported that the mixture of acrylic acid and allylamine in the plasma gas phase lead to the formation of an allylammonium acrylate salt, acting as a third monomer during the plasma polymerization. Hence, it appears difficult to predict the film composition issued from plasma copolymerization as some monomer interactions in the gas phase might or might not occur.

Figure 11 reports a plot of the DMA content in the film (i.e., F_{DMA}) as a function of DMA in the feed (f_{DMA}). First, it can be noticed that both XPS methods, based on the N content and C 1s curve fits, provided a good agreement in the F_{DMA} estimation. In addition, it was confirmed that F_{DMA} was lower than f_{DMA} as the curve was below the diagonal. As an example, the $D_{75}E_{25}$ film only contained a DMA amount of 0.27 molar fraction, while a 0.75 DMA amount was initially introduced in the feed. This result indicated that DMA monomer showed lower reactivity as compared to EGDMA, suggesting that EGDMA entered more in the copolymer structure than DMA. Here, the use of a pulsed plasma process, enabling the high retention of the monomer structure in the deposited film, justifies an interpretation of the observed nonlinear relationship between the feed and the film composition in correlation with conventional free-radical
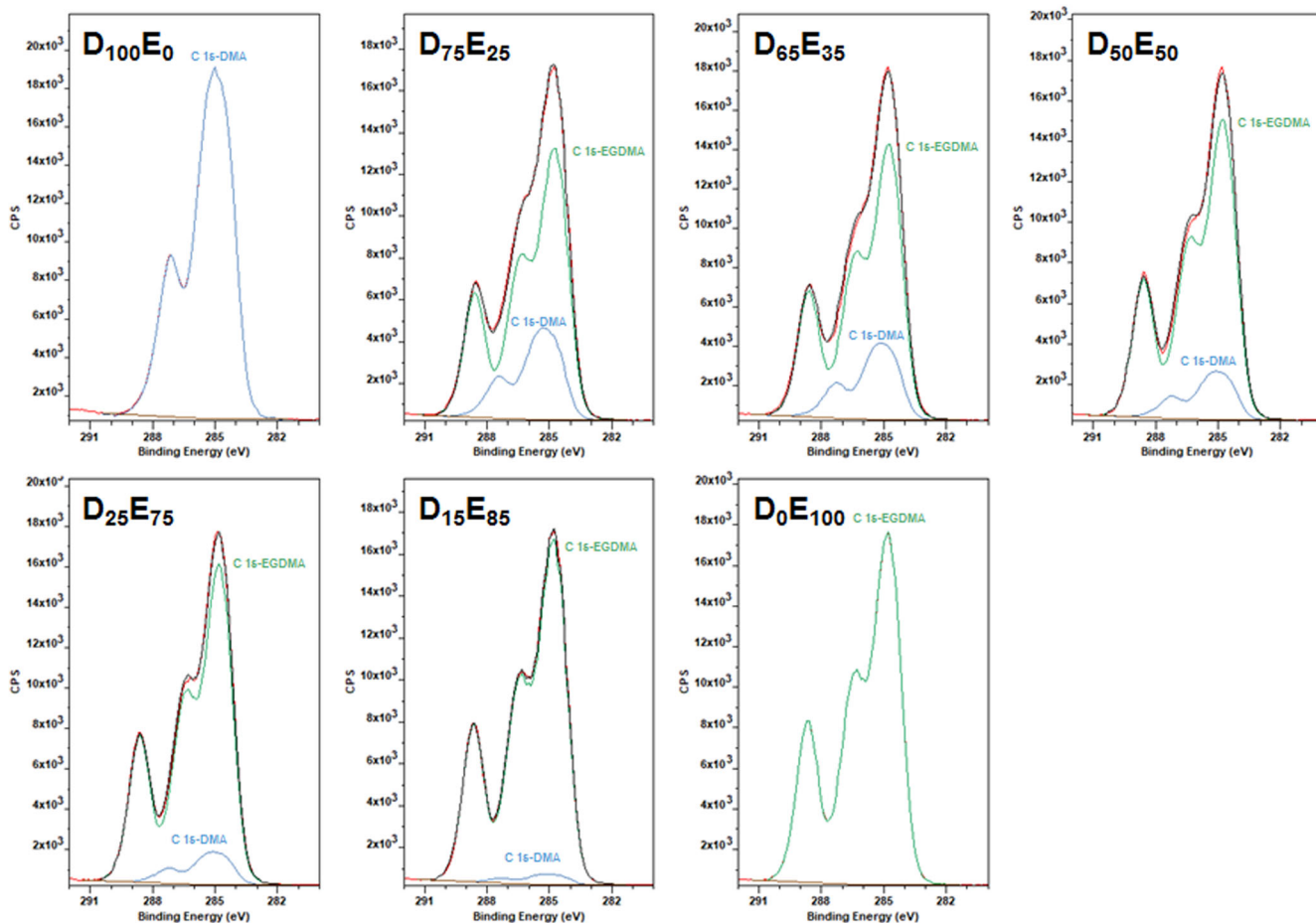
FIGURE 10 X-ray photoelectron spectroscopy C 1s curve fitting of plasma deposited films deposited from pure DMA ($D_{100}E_0$), EGDMA (D_0E_{100}) and different DMA–EGDMA compositions. DMA, *N,N*-dimethylacrylamide; EGDMA, ethylene glycol dimethacrylate
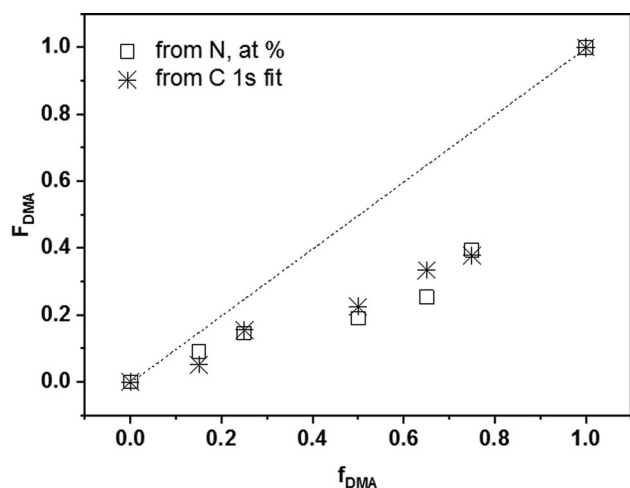

FIGURE 11 Plot of *N,N*-dimethylacrylamide (DMA) molar fraction in the film, estimated by X-ray photoelectron spectroscopy N 1s content and C 1s curve fitting, as a function of DMA molar fraction in the feed

mechanism.[31] Hence, in the work of Isaure et al.,[32] the authors reported that DMA could be copolymerized with EGDMA via conventional free-radical polymerization performed in solution. In particular, this copolymerization was characterized by reactivity ratios of 0.45 and 2.0 for DMA and EGDMA, respectively. The much higher reactivity ratio for EGDMA when compared to that for DMA indicated the preferential incorporation of EGDMA to all propagating radicals. As the mechanism of polymer growth in our plasma initiated process is assumed to be of the radical type, the observed enrichment of EGDMA in the plasma copolymers even at small EGDMA feed fractions is in line with these reactivity ratios.

The chemical structures of the copolymers were investigated by MALDI-HRMS analyses. As expected, the precursor feed presenting a high amount of EGDMA led to the formation of cross-linked films. Such films are not easily analyzed by MALDI-HRMS. Indeed, the ionization of the molecular species is particularly difficult, thus

TABLE 3 Main distributions detected by MALDI-HRMS analyses of atmospheric pulsed DMA/EGDMA plasma copolymerized films

Annotation	Copolymer structure	Repeating unit, n and m, for $D_{85}E_{15}$	Repeating unit, n and m, for $D_{75}E_{25}$
C_1		$m = 0$ and $1 \leq n \leq 7$	$m = 0$ and $2 \leq n \leq 6$
		$n = 1$ and $1 \leq m \leq 2$	$n = 1$ and $1 \leq m \leq 3$
		$n = 2$ and $1 \leq m \leq 3$	$n = 2$ and $1 \leq m \leq 3$
		$n = 3$ and $1 \leq m \leq 2$	$n = 3$ and $m = 1$
		$n = 4$ and $m = 1$	$n = 4$ and $m = 1$
		$n = 5$ and $m = 1$	
C_2		$m = 0$ and $1 \leq n \leq 6$	$m = 0$ and $1 \leq n \leq 6$
		$n = 1$ and $1 \leq m \leq 3$	$n = 1$ and $1 \leq m \leq 4$
		$n = 2$ and $1 \leq m \leq 2$	$n = 2$ and $1 \leq m \leq 2$
		$n = 3$ and $m = 1$	$n = 3$ and $m = 1$
C_3		$m = 0$ and $1 \leq n \leq 6$	$m = 0$ and $1 \leq n \leq 6$
		$n = 1$ and $1 \leq m \leq 3$	$n = 1$ and $1 \leq m \leq 3$
		$n = 2$ and $1 \leq m \leq 3$	$n = 2$ and $1 \leq m \leq 2$
		$n = 3$ and $m = 1$	$n = 3$ and $1 \leq m \leq 2$
		$n = 4$ and $m = 1$	$n = 4$ and $m = 1$
		$n = 5$ and $m = 1$	
C_4		$m = 0$ and $1 \leq n \leq 6$	$m = 0$ and $1 \leq n \leq 6$
		$n = 1$ and $1 \leq m \leq 3$	$n = 1$ and $1 \leq m \leq 2$
		$n = 2$ and $1 \leq m \leq 2$	$n = 2$ and $1 \leq m \leq 2$
		$n = 3$ and $1 \leq m \leq 2$	$n = 3$ and $1 \leq m \leq 2$
		$n = 4$ and $m = 1$	$n = 4$ and $m = 1$

Abbreviations: DMA, N,N-dimethylacrylamide; EGDMA, ethylene glycol dimethacrylate; HRMS, high-resolution mass spectroscopy; MALDI, matrix-assisted laser desorption/ionization.

limiting the detection of oligomer and/or polymer species. Therefore, in this study, only the results achieved for the $D_{85}E_{15}$ and $D_{75}E_{25}$ films are shown in Table 3.

In the previous section, MALDI-HRMS analyses revealed the presence of PDMA oligomer distributions with a DMA repeating unit (n) up to 11. Here, as shown in Table 3, DMA/EGDMA copolymers were detected with n up to 6 and an EGDMA repeating unit (m) up to 3.

Irrespective of the DMA/EGDMA precursor mixtures in the feed, SEM observations (Figure S2) revealed the formation of particle-free thin films. Complementary AFM analyses, carried out on 154 ± 36-nm thick coatings, indicated that the films presented an arithmetical mean height averaged (Sa) of around 3 nm (Figure S3).

Furthermore, film properties were investigated via water immersion tests for 1.5 hr and SEM observations. Hence, water-stable thin films were produced using EGDMA/DMA molar fraction superior or equal to 0.35 mol%. Indeed, the film thickness remained mostly unchanged after the immersion step (Figure 12a), suggesting the formation of cross-linked films. Complementary WCA measurements highlighted that the coatings presented similar wetting properties with WCA values of approximately 70°, close to the WCA value of a plasma polymer film from pure EGDMA (Figure S4). In addition, SEM observations did not reveal any crack in the layer after water immersion (Figure 12b) but highlighted the appearance of sparse circles and/or wrinkles, resulting
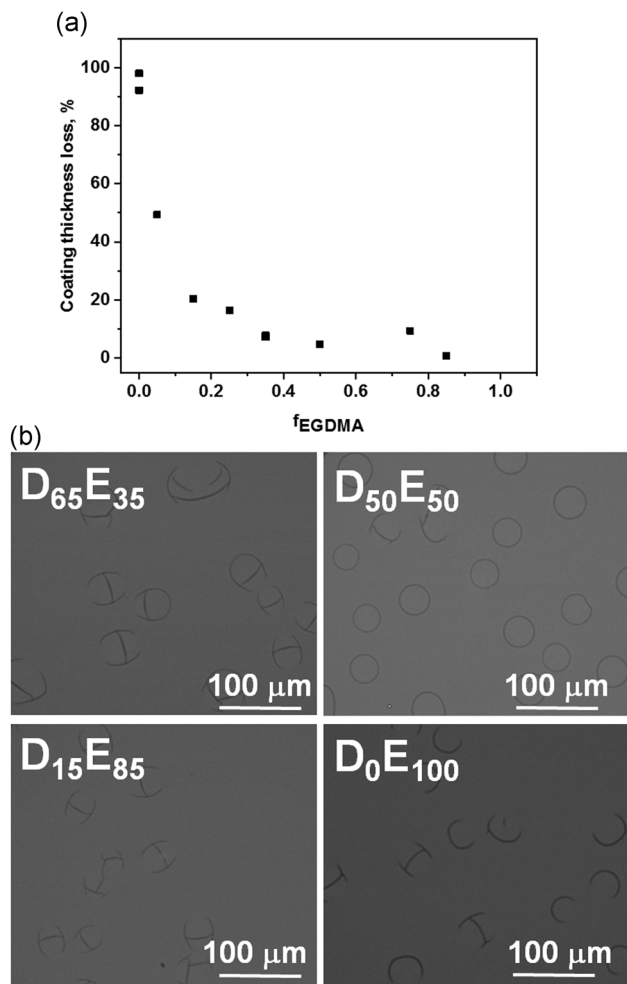
(a)

(b)

FIGURE 12 Evolution of the coating thickness loss (%) after water immersion for 1.5 hr as a function of the EGDMA content in the feed (f_{EGDMA}) (a) and SEM pictures of the copolymers films after immersion in water for 1.5 hr (b). EGDMA, ethylene glycol dimethacrylate; SEM, scanning electron microscopy

FIGURE 13 Cell metabolic activity for human mesenchymal stem cells cultured with extracts collected from silicon wafer substrates (Si) and $D_{15}E_{85}$ coated silicon wafer substrates ($D_{15}E_{85}$), and those cultured with only the culture media (blank) was found to be statistically different from those cultured with the cytotoxic control (phenol) ($p < .0001$). The dashed line represents the ISO 10993-5 limitation for acceptable cytotoxicity. ****A statistical difference between phenol and all other groups ($p < .0001$)

probably from water absorption into the film and its subsequent evaporation during the drying step. Finally, the chemistry of the copolymer films after water immersions (i.e., $D_{(1-x)}E_{(x>35)}$) was studied by FTIR analyses. Interestingly, no noticeable change was observed, thus confirming an excellent water and chemical stability (Figure S5).

In the previous section, water-stable DMA/EGDMA films were produced and might be used as matrices for DOMA incorporation to deposit water-stable catechol-bearing films. Before the exploitation of the coatings in biological applications, considering the known DMA toxicity (by skin contact and swallowing) and EGDMA allergic property (skin irritation, respiratory), the cytotoxicity of DMA/EGDMA films was investigated. Here, preliminary indirect toxicity tests were carried out using hMSCs and $D_{15}E_{85}$ films. Biological results, shown in
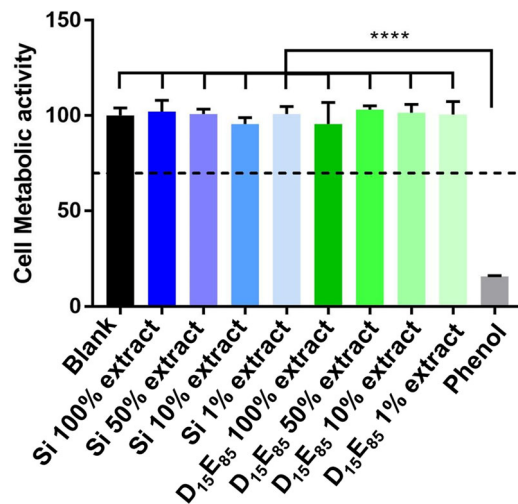
Figure 13, clearly demonstrate the nonalteration of the cell metabolic activity cultured in extracts issued from the plasma polymer films. Therefore, it can be concluded that there was no leaching of toxic compounds, such as low molecular weight compounds, from the plasma polymer films. The films were well cross-linked and noncytotoxic, thus paving the way to their exploitation as biointerfaces.

3.3 | Water-stable terpolymer plasma deposition for biological applications

To produce stable and yet chemically reactive interlayers for biomolecule immobilizations, thin films were produced from DOMA-$D_{50}E_{50}$ solution composed of 0.45×10^{-3} mol of DOMA and 12.1×10^{-3} mol of DMA and EGDMA. As shown in the UV spectra of the DOMA-$D_{50}E_{50}$ film (Figure 14a), the presence of a peak centered at 280 nm, attributed to the catechol group,[33] confirmed the good incorporation of DOMA in the deposited film. QCM-D analyses, reported in Figure 14b, indicated the efficient immobilization of lysozyme, pointed out by the frequency decreased (ΔF approximately -90 Hz) commonly attributed to a mass gain (i.e., lysozyme deposition on the sensor). The rinsing step induced an increase in the frequency (i.e, a mass loss) attributed to the removing of unbonded biomolecule, leading to a final frequency shift of -70 Hz. Interestingly,
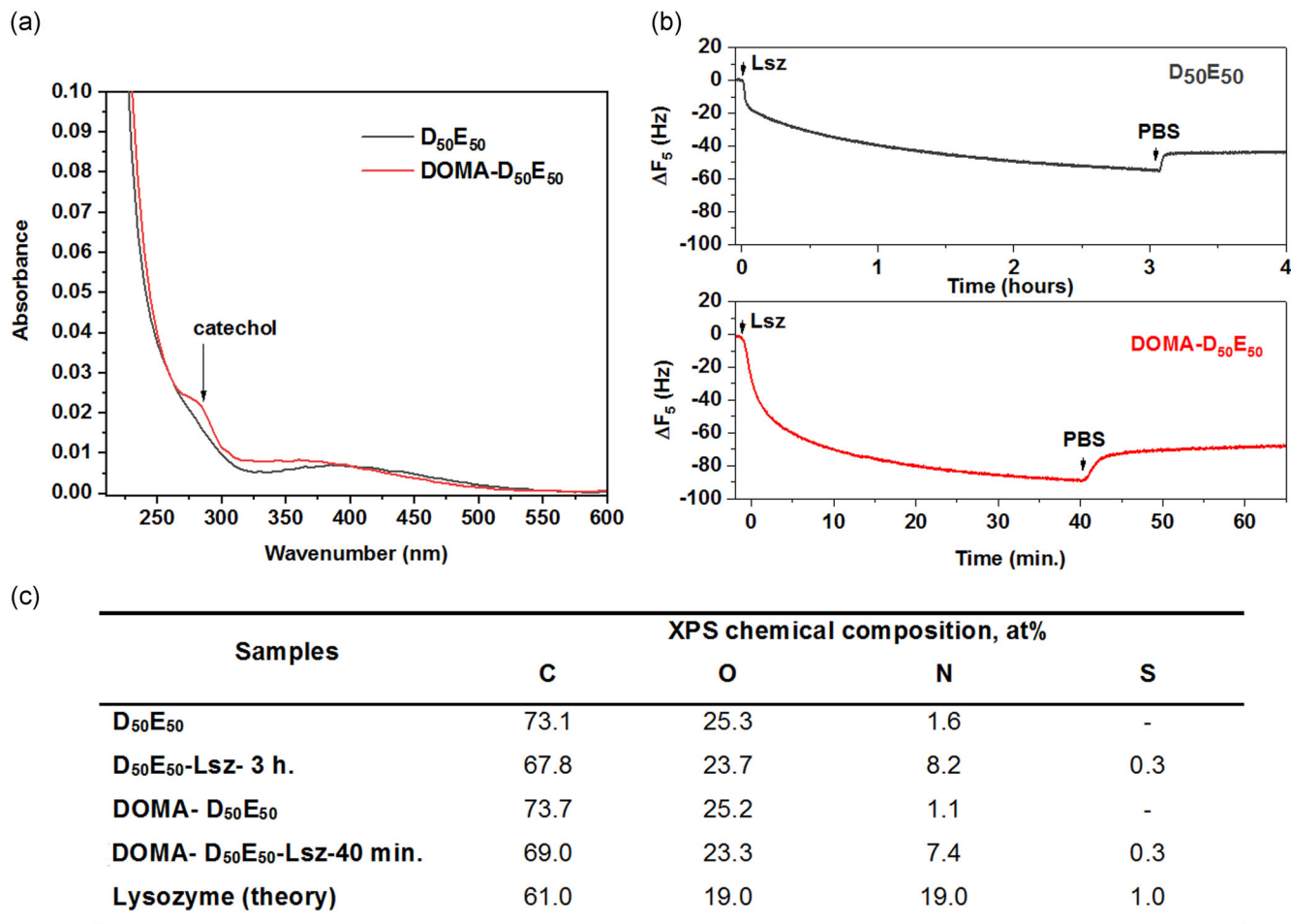
(a)

(b)

(c)

Samples	XPS chemical composition, at%			
	C	O	N	S
D$_{50}$E$_{50}$	73.1	25.3	1.6	-
D$_{50}$E$_{50}$-Lsz- 3 h.	67.8	23.7	8.2	0.3
DOMA- D$_{50}$E$_{50}$	73.7	25.2	1.1	-
DOMA- D$_{50}$E$_{50}$-Lsz-40 min.	69.0	23.3	7.4	0.3
Lysozyme (theory)	61.0	19.0	19.0	1.0

FIGURE 14 Ultraviolet spectra of DOMA-D$_{50}$E$_{50}$ and D$_{50}$E$_{50}$ plasma polymer films (a), quartz crystal microbalance with dissipation monitoring frequency shift of D$_{50}$E$_{50}$ and DOMA-D$_{50}$E$_{50}$ coated sensors with lysozyme (Lsz) introduction at time 0 (b), and X-ray photoelectron spectroscopy chemical composition of different plasma polymer films with and without lysozyme immobilization (c). DOMA, dopamine methacrylamide

the coated surface was fully saturated by lysozyme in only 8 min. As controls, QCM-D experiments were carried out using D$_{50}$E$_{50}$-coated sensors. The introduction of lysozyme was also accompanied by a frequency decrease (ΔF approximately -50 Hz), indicating the biomolecule immobilization. It is worth noting that the stabilization of the baseline was achieved after 3 hr versus 40 min. using DOMA-D$_{50}$E$_{50}$ coated sensors. In addition, the rinsing step induced an increase in the frequency shift (i.e., removal of biomolecule) to reach a final ΔF value of approximately -40 Hz. Hence, the kinetic of immobilization of the lysozyme onto D$_{50}$E$_{50}$ coated surfaces was estimated to be around 2 hr. After the QCM-D measurements, the sensors were analyzed by XPS analyses (Figure 14c). Irrespective of the coating nature, an increase in the nitrogen amount (by approximately a factor of 7) at the surface was observed. The presence of sulfur was also detected. Such elements being part of the lysozyme amino acid sequence, the immobilization of lysozyme surfaces was confirmed. However, the long kinetic of reactions associated to the smaller frequency shift achieved for the D$_{50}$E$_{50}$ coatings, compared to the DOMA-D$_{50}$E$_{50}$ films, tended to suggest that the chemical nature of the biomolecule immobilization was different in each case. Indeed, considering the hydrophobic character of the D$_{50}$E$_{50}$ films, the biomolecule immobilization might be explained by strong hydrophobic surface-hydrophobic protein interactions. In contrast, considering both the DOMA-D$_{50}$E$_{50}$ film nature and the pH solution used for immobilization, the covalent bonding of lysozyme onto the plasma layer might reasonably be assumed. Indeed, the Schiff base formation and/or the Michael addition reactions might have occurred via the free amino group from lysozyme and the catechol/quinone chemistry from the coating. Such bioconjugation route is particularly interesting considering that neither

the surface nor the biomolecule requires an activation step and that the rate of grafting is fast.

4 | CONCLUSION

In this study, water-stable catechol-bearing plasma polymers films were successfully produced from an atmospheric pulsed plasma polymerization using a DOMA/DMA/EGDMA precursor mixture composed of a 0.129 mol/ml DOMA concentration in a 50–50 mol% DMA/EGDMA solution. With this objective, the growth mechanism of atmospheric pulsed plasma deposited DMA/EGDMA films, at 30 W using a 1 ms t_{on} and 60 ms t_{off}, was elucidated by combining kinetic studies and surface- and volume-sensitive techniques. Importantly, XPS analyses highlighted that the plasma feed composition drastically differed from the film composition, with the preferential incorporation of EGDMA in the coating. Hence, as an example, the formation of water-stable DMA–EGDMA coating was achieved by using a $D_{50}E_{50}$ mixture. Such feed composition led to the formation of a film containing only 20 mol% of DMA and 80 mol% of EGDMA according to the XPS quantification methods based on the C 1s curve fit and the N 1s elemental content. Interestingly, preliminary indirect biological tests confirmed the noncytotoxicity of DMA/EGDMA plasma matrix. Finally, pulsed plasma deposited catechol-bearing films, based on DMA/EGDMA copolymers, were able to efficiently immobilized lysozyme, used in this case as model molecule. In the future, efforts will be focused on the exploitation of such single and dry route in combination with the proper selection of active biomolecules for different biological purposes.

ORCID

Maryline Moreno-Couranjou http://orcid.org/0000-0003-0041-5532

REFERENCES

[1] *CVD Polymers: Fabrication of Organic Surfaces and Devices* (Ed: K. K. Gleason), Wiley, Weinheim, Germany **2015**.

[2] A. Manakhov, M. Moreno-Couranjou, N. D. Boscher, P. Choquet, J. Pireaux, *Plasma Processes Polym.* **2012**, *9*, 435.

[3] G. Camporeale, M. Moreno-Couranjou, N. D. Boscher, C. Bebrone, R. Mauchauffé, V. De Weerdt, H. Cauchie, P. Favia, P. Choquet, *Plasma Processes Polym.* **2015**, *12*, 1208.

[4] J. Friedrich, *Plasma Processes Polym.* **2011**, *8*, 783.

[5] M. Veuillet, L. Ploux, A. Airoudj, Y. Gourbeyre, E. Gaudichet-Maurin, V. Roucoules, *Plasma Processes Polym.* **2017**, *14*, 1.

[6] M. Vandenbossche, J. Dorst, M. Amberg, U. Schütz, P. Rupper, M. Heuberger, D. Hegemann, *Polym. Degrad. Stab.* **2018**, *156*, 259.

[7] L. J. Ward, W. C. E. Schofield, J. P. S. Badyal, *Chem. Mater.* **2003**, *15*, 1466.

[8] M. Moreno-Couranjou, P. Choquet, J. Guillot, H.-N. Migeon, *Plasma Processes Polym.* **2009**, *6*, S397.

[9] C. P. Klages, K. Höpfner, N. Kláke, R. Thyen, *Plasmas Polym.* **2000**, *5*, 79.

[10] F. Loyer, G. Frache, P. Choquet, N. D. Boscher, *Macromolecules* **2017**, *50*, 4351.

[11] R. Förch, Z. Zhang, W. Knoll, *Plasma Processes Polym.* **2005**, *2*, 351.

[12] S. Swaraj, U. Oran, J. F. Friedrich, A. Lippitz, W. E. S. Unger, *Plasma Processes Polym.* **2007**, *4*, 376.

[13] U. Czuba, R. Quintana, M. Bourguignon, M. Moreno-Couranjou, M. Alexandre, C. Detrembleur, P. Choquet, *Adv. Healthcare Mater.* **2018**, *7*, 1701059.

[14] M. Macgregor, K. Vasilev, *Materials* **2019**, *12*, 191.

[15] B. R. Coad, M. Jasieniak, S. S. Griesser, H. J. Griesser, *Surf. Coat. Technol.* **2013**, *233*, 169.

[16] R. Mauchauffé, M. Moreno-Couranjou, N. D. Boscher, A. Duwez, P. Choquet, *Plasma Processes Polym.* **2016**, *13*, 843.

[17] H. Lee, J. Rho, P. B. Messersmith, *Adv. Mater.* **2009**, *21*, 431.

[18] B. Akhavan, M. Croes, S. G. Wise, C. Zhai, J. Hung, C. Stewart, M. Ionescu, H. Weinans, Y. Gan, S. Amin, M. M. M. Bilek, *Appl. Mater. Today* **2019**, *16*, 456.

[19] D. Hegemann, I. Indutnyi, L. Zají, E. Makhneva, M. Vandenbossche, *Plasma Processes Polym.* **2018**, *15*, 1800090.

[20] F. Barletta, A. Liguori, C. Leys, V. Colombo, M. Gherardi, A. Nikiforov, *Mater. Lett.* **2018**, *214*, 76.

[21] D. Ben Salem, O. Carton, H. Fakhouri, F. Arefi-khonsari, *Plasma Processes Polym.* **2014**, *11*, 269.

[22] U. Czuba, R. Quintana, P. Lassaux, R. Bombera, G. Ceccone, J. Bañuls-Ciscar, M. Moreno-couranjou, C. Detrembleur, P. Choquet, *Colloids Surf., B* **2019**, *178*, 120.

[23] C. Amorosi, C. Mustin, G. Frache, P. Bertani, A. Fahs, G. Francius, V. Toniazzo, D. Ruch, V. Ball, L. Averous, M. Michel, *J. Phys. Chem. C* **2012**, *116*, 21356.

[24] F. Loyer, A. Combrisson, K. Omer, M. Moreno-Couranjou, P. Choquet, N. D. Boscher, *ACS Appl. Mater. Interfaces* **2018**, *11*, 1335.

[25] K. Lachmann, M. C. Rehbein, M. Jänsch, M. Thomas, C.-P. Klages, *Medicine* **2012**, *2*, 127.

[26] V. Jalaber, D. Del Frari, J. De Winter, K. Mehennaoui, S. Planchon, P. Choquet, C. Detrembleur, M. Moreno-Couranjou, *Front. Chem.* **2019**, *7*, 1.

[27] A. Carletto, J. P. S. Badyal, *Phys. Chem. Chem. Phys.* **2019**, *21*, 16468.

[28] J. Mertens, J. Baneton, A. Ozkan, E. Pospisilova, B. Nysten, A. Delcorte, F. Reniers, *Thin Solid Films* **2019**, *671*, 64.

[29] D. Beamson, G. Briggs, *High Resolution XPS of Organic Polymers: The Scienta ESCA 300 Database*, Wiley-VCH, Weinheim, Germany **1992**.

[30] A. J. Beck, J. D. Whittle, N. A. Bullett, P. Eves, S. Mac Neil, S. L. Mcarthur, A. G. Shard, *Plasma Processes Polym.* **2005**, *2*, 641.

[31] M. Finemann, S. D. Ross, *J. Polym. Sci.* **1950**, *5*, 259.

[32] F. Isaure, P. A. G. Cormack, D. C. Sherrington, *React. Funct. Polym.* **2006**, *66*, 65.

[33] M. Yu, J. Hwang, T. J. Deming, *J. Am. Chem. Soc.* **1999**, *121*, 5825.

SUPPORTING INFORMATION

Additional supporting information may be found online in the Supporting Information section.